Int. J. Heat Mass Transfer. Vol. 30, No. 2, pp. 395–400, 1987
Printed in Great Britain

0017–9310/87 $3.00 + 0.00
Pergamon Journals Ltd.

TECHNICAL NOTES

Simultaneous heat and mass transfer between a fluidized bed of fine particles and immersed coarse porous particles

S. COBBINAH, C. LAGUÉRIE* and H. GIBERT
E.N.S.I.G.C., Chemin de la Loge, 31078 Toulouse Cédex, France

(*Received* 3 *January* 1986 *and in final form* 5 *May* 1986)

1. INTRODUCTION

FLUIDIZATION techniques have been applied in recent years to a wider range of operations (e.g. solids drying, ore roasting, gasification and pyrolysis of solid fuels) than the traditional catalytic cracking processes and non-isothermal gas–solid reactions. New fields of application of fluidization quite often involve coarse solid particles ($d_p > 1.0$ mm) with poor fluidization qualities and ineffective gas–solid contact. This explains the development of more appropriate non-classical fluidization techniques amongst which that of immersion of the coarse, active solids in a high-quality fluidized medium of fine and inert particles promises to offer wide industrial applications. This work is aimed at a better understanding of the heat and mass transfer phenomena underlying such a technique by means of an experimental approach based on the constant rate period drying of moist, porous alumina spheres in air fluidized beds of sand particles.

2. HEAT AND MASS TRANSFER MECHANISMS

2.1. *Heat transfer*

The heat flux to the wet surface of the alumina spheres, like bed-to-wall heat exchange [1, 2] at low temperatures may be considered as the resultant of two contributions.

(a) A gas-convective flux, q_c, from the hot fluidizing gas to the moist solids across a thin film of stagnant gas adjacent to the evaporating surface.

This may be defined by:

$$q_c = h_c(T_g - T_s) \tag{1}$$

where h_c is the gas-convective heat transfer coefficient, T_g the bulk gas temperature and T_s the surface temperature of the moist particles.

(b) An interparticle heat flux induced by the temperature difference between the moist particles and the hot fluidized fine particles. Like the particle-induced convective component in bed-to-wall heat transfer [1] this is considered to occur by the release of heat to the stagnant gas film surrounding the moist surface by the hot fine particles during their intermittent contact with the coarse particles [3, 4]. The interparticle heat flux, q_p, can be defined by:

$$q_p = h_p(T_p - T_s) \tag{2}$$

where h_p is the interparticle heat transfer coefficient and T_p the fine particle temperature.

From equations (1) and (2), the total heat flux can be written as:

$$q_t = h_c(T_g - T_s) + h_p(T_p - T_s). \tag{3}$$

A mean solid temperature $\bar{T}_p$ can be defined in the bed [5, 6] by:

$$\bar{T}_p = fT_p + (1-f)T_s \tag{4}$$

where f is the mass fraction of the fine particles in the bed.

The high values of f ($=0.98$) used in this work permit a reasonable approximation from equation (4):

$$\bar{T}_p = T_p. \tag{5}$$

Owing to the high specific area of the fluidized particles one may consider that the gas–solid heat exchange is confined to a small zone above the distributor. In other words, a gas–solid thermal equilibrium can be assumed, hence:

$$\bar{T}_p = T_p = T_g. \tag{6}$$

Substitution of equation (3) yields:

$$q_t = h_t(T_g - T_s) \tag{7}$$

where h_t is the total heat transfer coefficient given by:

$$h_t = h_p + h_c. \tag{8}$$

2.2. *Mass transfer*

Since the fine particles are non-porous, water vapor transfer from the evaporating surface occurs by convection only. The flux, N, is defined by:

$$N = k(H_s - H_g) \tag{9}$$

where k is the mass transfer coefficient, H_s the absolute humidity of gas in contact with the wet surface and H_g the bulk gas absolute humidity.

3. EXPERIMENTAL APPARATUS AND PROCEDURES

The experimental set-up (Fig. 1) consisted essentially of a stainless-steel, rectangular cross-sectional column ① ($120 \times 360 \times 600$ mm) containing a bed of fine sand (80 mm high) supported on a perforated plate distributor (hole diameter of 1 mm with a rectangular pitch of 80 mm).

The wet, porous alumina spheres were contained in a basket ② suspended a few millimetres ($\simeq 30$ mm) above the distributor. The basket holes were large enough to allow the free movement of the fine particles. This arrangement was to ensure that the drying occurs only in the isothermal zone, i.e. where equation (6) holds.

Bed temperature was maintained at a prefixed value by means of a feedback system comprising an iron–constantan thermocouple ⑦ inserted in the bed, a Philips P.I.D. temperature recorder controller ④ and a 12-kW electric coil air heater ③.

Fluidizing air humidity was measured by means of a dew point LiCl probe ⑩ and counterchecked with wet- and dry-bulb psychrometer measurements (maximum difference of 10%).

The experimental runs consisted in determining the drying rate of the alumina spheres fed into the fluidized bed of fine sand maintained at a fixed temperature. To ensure the appearance of a measurable constant rate period, it was

NOMENCLATURE

A surface area [m^2]
C_{ph} specific heat of humid air [J (kg dry air)$^{-1}$ °C^{-1}]
d_L large particle diameter [m]
$\bar{d}_p$ mean fine particle size [m]
D diffusivity of water vapor in air [m^2 s^{-1}]
g gravitational acceleration [m s^{-2}]
G gas mass flow rate [kg m^{-2} h^{-1}]
h_c gas convective heat transfer coefficient [W m^{-2} °C^{-1}]
h_p interparticle heat transfer coefficient [W m^{-2} °C^{-1}]
h_t total heat transfer coefficient [W m^{-2} °C^{-1}]
H_g absolute humidity of bulk gas [(kg water) (kg dry air)$^{-1}$]
H_s absolute humidity of air in contact with moist surface [(kg water) (kg dry air)$^{-1}$]
k convective mass transfer coefficient based on humidity difference [kg m^{-2} s^{-1} ΔH^{-1}]
R drying rate [(kg water evaporated)(kg dry solid s)$^{-1}$]
T_g bulk gas temperature [°C]
T_p fine particle temperature [°C]
$\bar{T}_p$ mean bed temperature [°C]
T_s surface temperature of moist particles [°C]
T_w wet-bulb temperature of air [°C]
U_{mf} minimum fluidization velocity of fine particles [m s^{-1}]
U_{mc} critical gas velocity [m s^{-1}].

Dimensionless groups
Ar Archimedes number, $gd_p^3(\rho_p-\rho_g)\rho_g/\mu_g^2$
J_D Chilton–Colburn factor for mass transfer, $(k/G)Sc^{2/3}$
J_H Chilton–Colburn factor for heat transfer, $(h/GC_{ph})Pr^{2/3}$
Le Lewis number, $(Sc/Pr)^{2/3}$
Nu Nusselt number, hd_L/λ_g
Pr Prandtl number, $\mu_g C_{ph}/\lambda_g$
Re_{mc} critical Reynolds number, $U_{mc}d_L\rho_g/\mu_g$
Sc Schmidt number, $\mu_g/\rho_g D$
Sh Sherwood number, kd_L/D.

Greek symbols
ρ_g gas density [kg m^{-3}]
ρ_p fine particle density [kg m^{-3}]
μ_g gas viscosity [kg m^{-1} s^{-1}]
λ_g gas thermal conductivity [W m^{-1} °C^{-1}].

imperative to saturate initially the alumina spheres with water and to conduct the drying experiments at temperatures not exceeding 20°C.

The slope of the sample moisture content–time plot in a given run was a measure of the drying rate expressed in kg water evaporated per kg dry solid per second. The first few minutes of each run were discarded in the graphical determination of the drying rate in order to avoid any misleading errors due to the overlapping of the initial drying period and the constant rate period. Relevant solid properties and ranges of experimental variables (d_L, d_p and U) are summarized in Table 1.

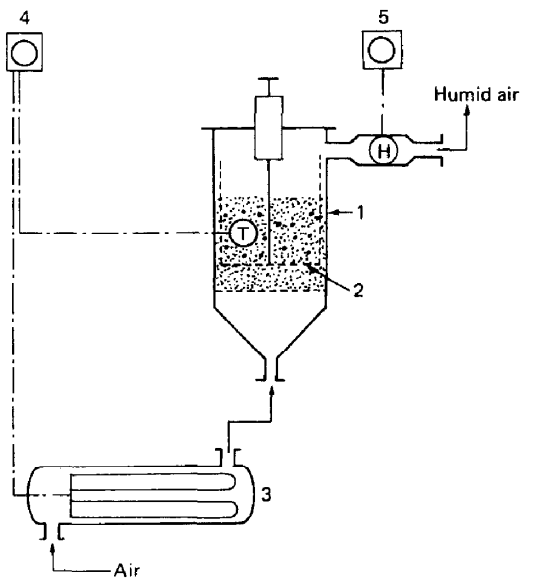

FIG. 1. Experimental setup: 1, fluidization column; 2, suspended basket; 3, air-preheater; 4, temperature recorder controller; 5, humidity recorder; H, hygrometer; T, thermocouple.

4. CALCULATION OF TRANSFER COEFFICIENTS AND SURFACE OF WET PARTICLES

From the measured drying rate R and the heat and mass transfer flux equations (7) and (9), respectively, the following overall energy and mass balances can be written:

$$\left|\begin{array}{c}\text{Heat required for}\\ \text{evaporation}\end{array}\right| = \left|\begin{array}{c}\text{sensible heat supplied to the wet surface}\\ \text{by convective and interparticle transfer modes}\end{array}\right|$$

$$R\Delta H_V = h_t A(T_g - T_s) \quad (10)$$

$$|\text{drying rate}| = |\text{convective mass transfer rate}|$$

$$R = kA(H_s - H_g). \quad (11)$$

Transfer coefficients h_t and k can thus be evaluated from equations (10) and (11), respectively, if the surface conditions T_s and H_s are known. It is well established that surface temperature of solids undergoing drying in the constant rate period is virtually equal to the wet-bulb temperature of the drying fluid when the heat supply is solely by convection. In the present work, the wet surface receives heat from the fluidized fine particles as well. T_s is thus likely to be higher than T_w as revealed in previous studies [6, 7].

By means of the arrangement illustrated in Fig. 2, the surface temperature of wet alumina spheres fixed in fluidized beds of fine sand were measured. The experimental conditions and variables were identical to those of the drying experiments (Table 1). The deviation of the measured surface temperature, T_{sm}, from T_w, represented by the ratio $(T_{sm}-T_w)/(T_p-T_w)$ was found to decrease as U/U_{mf} increases (Figs. 3 and 4) for all combinations of d_L and D_p. At a given U/U_{mf}, it is apparently independent on d_L (Fig. 3) but decreases as the fluidized particles become coarser (Fig. 4). Vanderschuren and Delvosalle [6] reported similar evolutions and a maximum deviation of 25% in the transfer potential in their experimental ranges: $1.5 < U/U_{mf} < 3.5$; $3.0 < d_L < 11.4$ mm and $0.79 < d_p < 5.70$ mm.

Table 1. Solid properties and ranges of experimental variables

Granulometry (μm)	$\bar{d}_p$ (μm)	U_{mf} (m s^{-1})
Inert fluidized medium of sand $\rho_p = 2650$ kg m^{-3}		
250–315	282.5	0.090
400–500	450	0.143
630–710	670	0.201

Porous alumina sphere

d_L (mm)	ρ_L (kg m^{-3})
5.0	1340
6.0	1350
8.4	1370

Fluidization velocity: $U_{mf} < U < 4U_{mf}$.

One may attempt to substitute the measured wet surface temperature of fixed particles, T_s, for T_w in equation (10) in order to obtain more exact values for h_t which in actual fact concerns mobile bodies. In our opinion this would rather be erroneous and would tend to mask the influence of the bed hydrodynamics on h_t. Our experimental results show clearly that the temperature deviation is a function of the hydrodynamic state of the bed: $(T_s - T_w)/(\bar{T}_p - T_w)$ decreases as U/U_{mf} increases (Figs. 3 and 4). In more fundamental terms, the closeness of T_s and T_w depends on the relative velocity between the large and fine particles which is obviously lower for mobile large bodies at a given fluidization velocity.

A useful significance can, however, be given to the measured deviation for fixed particles on considering the interparticle heat transfer as resulting from the transient heat transfer between the cold surface and the fluidized particles [4, 10] during their intermittent contact. The importance of the interparticle transfer depends on the frequency of the renewal or the residence time of the fine particles at the cold transfer surface. It is known [3, 4, 10] that frequency renewal of the transfer surface (low residence time of fluidized particles) results in high temperature gradients and consequently promotes the interparticle transfer. It follows by a comparison between the fixed and mobile particles cases that the interparticle transfer, hence the temperature deviation, would be lesser in the latter case since the relative velocity between the large and fluidized fine particles is lower. The temperature deviation obtained for the fixed particle case can thus be regarded as the upper limit of that of the mobile particle case.

In spite of the observed deviation of T_s from T_w it appeared preferable to evaluate h_t from the assumption that T_s is equal to T_w for the following reasons: (i) although the h_t values given by this procedure are conservative, they give an adequate picture of the relationship between the transfer phenomena and the bed hydrodynamics. Such information is vital for the understanding of the transfer mechanism, which is our primary aim here; (ii) the conservative coefficients can be safely used for design purposes. In the case of a rigourous design, a correction factor taking into account the deviation of T_s from T_w can be applied. Work is going on in our laboratory in this direction and the results will be published soon.

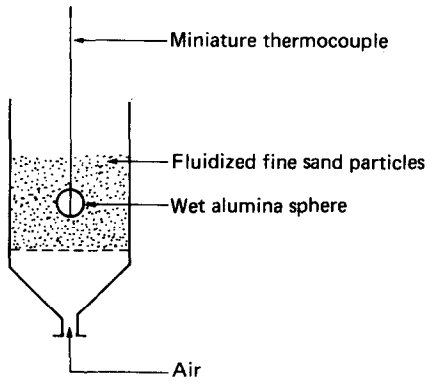

FIG. 2. Experimental setup for measuring the surface temperature of wet particles.

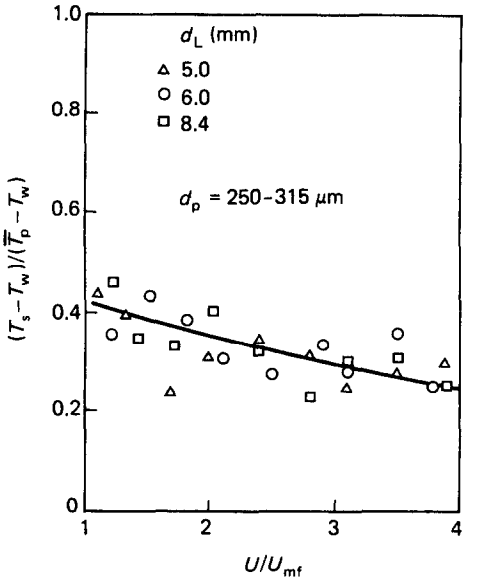

FIG. 3. Deviation of measured wet surface temperature from wet-bulb temperature: effect of large particle size.

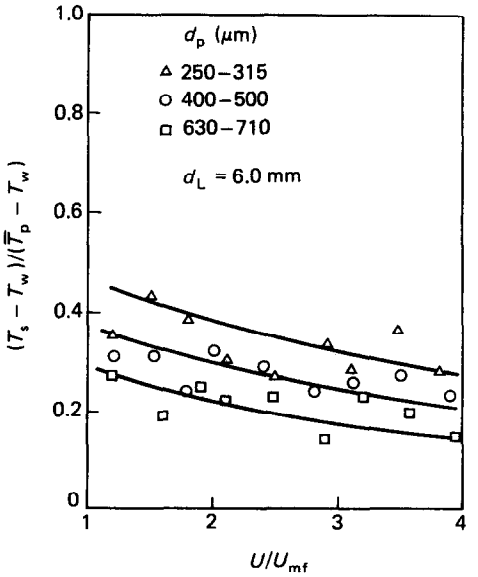

FIG. 4. Deviation of measured wet surface temperature from wet-bulb temperature: effect of fine particle size.

5. RESULTS AND DISCUSSION

5.1. *Hydrodynamic behaviour*

All the binary systems (defined d_L and d_p) investigated exhibit two distinct hydrodynamic regimes with corresponding k–U and h_t–U relationships. At low gas velocities between the minimum fluidization velocity and a certain critical value, U_{mc}, the coarse particles remain practically immobile in an incipient bubbling bed. This state of complete solid segregation is described by Rios and Gilbert [8] as the static regime. In the high gas velocity range ($U_{mc} < U < 4U_{mf}$), the coarse particles move freely in a well-developed bubbling bed. Like the previous studies [9] on the mixing and segregation phenomena in binary systems, the large and fast bubbles which appear more frequently at this stage are considered as the agents responsible for the large particle circulation. This state is referred to [8] as the dynamic regime.

Experimental data on the critical gas velocity could be fitted by the correlation:

$$Re_{mc} = 4.331 \times 10^{-3} Ar^{0.732} (d_L/d_p)^{1.332}. \quad (12)$$

Considering the randomness and the rapidity of the circulation of the large particles in the dynamic regime one can envisage that the local conditions are uniform on the entire transfer surface. This justifies the definition of an average transfer coefficient between the bed and the immersed large particles based on the uniform surface conditions T_s and H_s. Such uniform surface conditions cannot obviously be admitted in the static regime which can in fact be likened to a 'packed bed of large particles' in a fluidized medium. The interpretation of the experimental data in this regime remains quite delicate. The quantitative treatment and interpretation of our raw experimental data were thus limited to the dynamic regime which in fact is of more practical interest.

5.2. *Mass transfer*

The mass transfer coefficient for a given binary system increases with the reduced superficial gas velocity U/U_{mf} (Figs. 5 and 6) in the static regime and assumes an almost constant value, k_{max}, in the dynamic regime. This behaviour

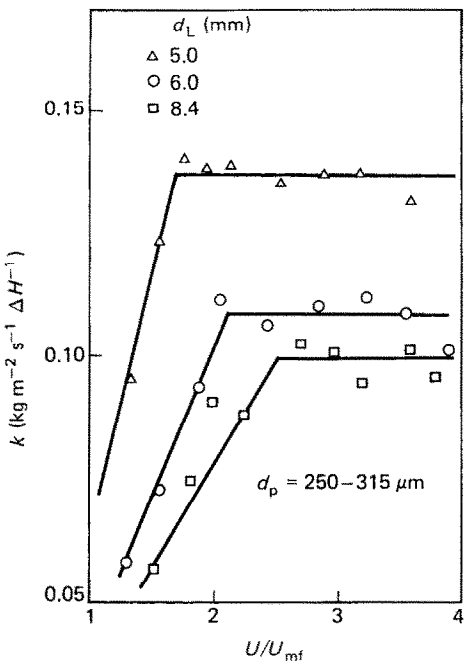

FIG. 5. Variation of mass transfer coefficient with reduced superficial gas velocity: effect of large particle size.

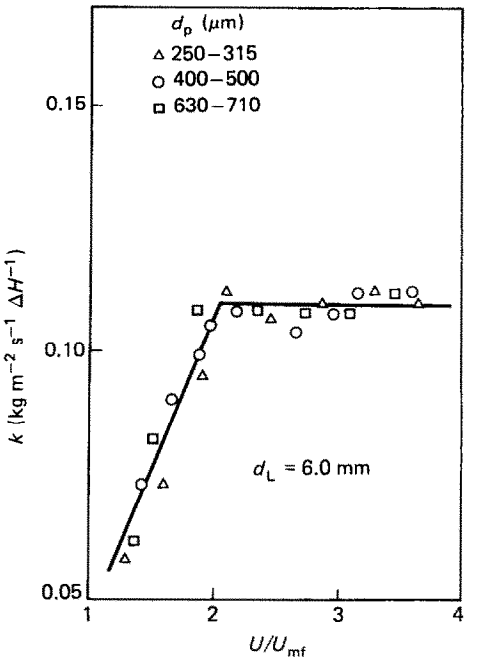

FIG. 6. Variation of mass transfer coefficient with reduced superficial gas velocity: effect of fine particle size.

is in good agreement with previous studies [10, 11] on large bodies fixed in fluidized beds of fine particles.

Furthermore, the mass transfer intensity increases markedly as the large particle size decreases (Fig. 5) but shows no apparent dependence on the fine particle size (Fig. 6). Experimental data on the effect of the large particle size on the maximum mass transfer coefficients were correlated by means of the equation:

$$k_{max} = 4.972 \times 10^{-3} d_L^{-0.617}. \quad (13)$$

The fine particles, through their action as turbulence promotors on the transfer surface, enhance the convective transfer in such binary systems compared to single-sized large particle systems [12].

5.3. *Total heat transfer*

The variation of the total heat transfer intensity with the reduced superficial gas velocity (Figs. 7 and 8) was found to be similar to that of the convective mass transfer: h_t is an increasing function of U/U_{mf} in the static regime but nearly constant in the dynamic regime. Similar h–U relationships have been reported for large mobile [9] and fixed [10, 11, 13] bodies in beds of fine particles.

The transfer coefficient increases appreciably with decreasing large particle size (Fig. 7) but to a lesser extent with the fine particle size. In the dynamic regime, this variation can be represented by the correlation:

$$h_{t,max} = 2.923 d_L^{-0.503} \bar{d}_p^{-0.140} \quad (14)$$

where $h_{t,max}$ is the maximum transfer coefficient.

The stronger influence of d_L suggests a predominance of the convective mechanism over the interparticle heat transfer mode; d_L is the primary factor governing the convective transfer as shown in the case of convective mass transfer.

The experimental data were also fitted by a dimensionless correlation showing in particular the effect of Archimedes number on $h_{t,max}$:

$$Nu_{max} = 3.25 Ar^{0.104} (d_L/\bar{d}_p)^{0.464}. \quad (15)$$

The above equation is valid for:

$$2 \times 10^3 < Ar < 3 \times 10^4 \quad \text{and} \quad 8 < d_L/\bar{d}_p < 30.$$

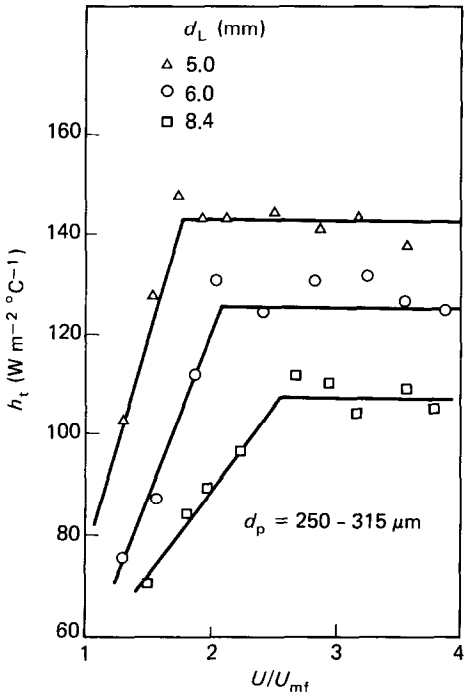

FIG. 7. Variation of total heat transfer coefficient with reduced superficial gas velocity: effect of large particle size.

It is worth noting that Nu_{max} is an increasing function of Ar as it is for bed-to-wall heat exchange [1, 2]. The dependence of Nu_{max} on Ar is, however, less pronounced in the studied system; the exponent of Ar in similar correlations for bed-to-wall transfer lies between 0.2 and 0.25 [2].

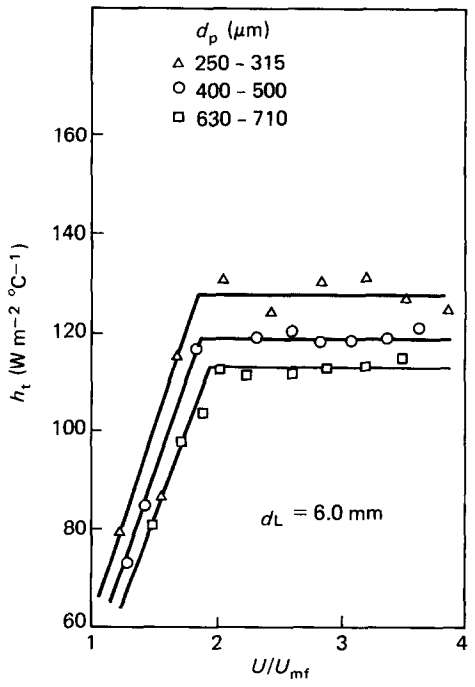

FIG. 8. Variation of total heat transfer coefficient with reduced superficial gas velocity: effect of fine particle size.

5.4. *Interparticle and gas convective heat transfer*

The individual heat transfer components in simultaneous heat and mass transfer studies may be evaluated [6, 10] on the basis of the non-absorptivity of the fine particles for water vapor and the assumption of analogous gas convective heat and mass transfer mechanisms. Quantitatively, this analogy is given by the equality of the Chilton–Colburn factors for heat and mass transfer:

$$J_H = J_D \tag{16}$$

$$\frac{h_c}{GC_{ph}} \cdot Pr^{2/3} = \frac{k}{G} \cdot Sc^{2/3} \tag{17}$$

which on simplification yields:

$$h_c = C_{ph}(Sc/Pr)^{2/3} = kC_{ph}Le^{2/3} \tag{18}$$

where C_{ph} is the specific heat of humid air.

For air–water systems at low humidity the factor $C_{ph}Le^{2/3}$ is known to be virtually constant. Under our working conditions ($15 < T < 20$°C and $6 < H_g < 10$ g/kg dry air) it varies between 909 and 913 J kg^{-1} °C^{-1}. The product of this nearly constant factor and the experimentally determined k value [equation (18)] gives an approximate estimation of h_c which can be derived from the corresponding h_t to obtain h_p.

The behaviour of the convective heat transfer coefficient with respect to the experimental variables (U/U_{mf}, d_L, d_p) was found to be identical to that exhibited by the convective mass transfer. This is a direct consequence of the analogy assumed in the computational procedure.

The interparticle heat transfer coefficient undergoes a slight and progressive fall as U/U_{mf} increases in the entire investigated range (Fig. 9). As for the falling branch of the h–U curves for the particle induced bed-to-wall heat exchange component [1, 2], this can be attributed to a decrease in the fine particle population density (increase in bed porosity) at the wet surface as U increases.

Besides, h_p increases as d_p decreases (Fig. 9) like bed-to-wall heat exchange. Experimental data on the variation of

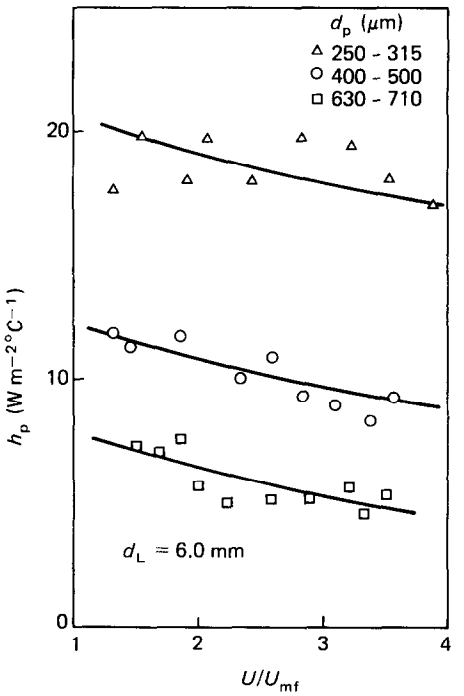

FIG. 9. Variation of the interparticle heat transfer coefficient with the reduced superficial gas velocity: effect of fine particle size.

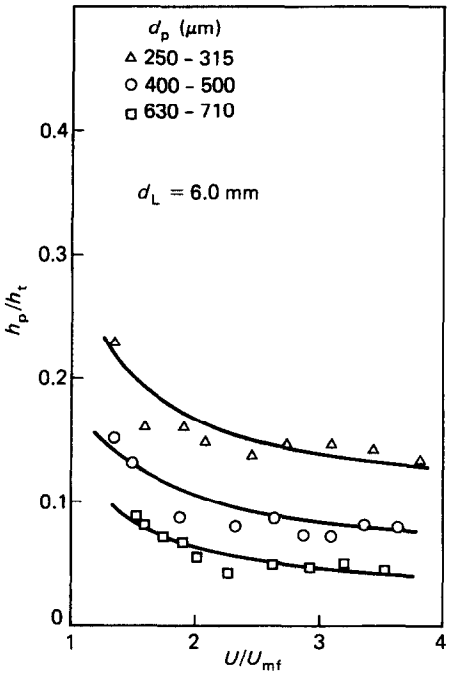

FIG. 10. Variation of the contribution of the interparticle heat transfer to the overall heat transfer: effect of fine particle size.

h_p with d_p and U/U_{mf} were fitted by the correlation:

$$h_p = 5.564 \times 10^{-4} \bar{d}_p^{-1.289} \left(\frac{U}{U_{mf}}\right)^{-0.167}. \quad (19)$$

The contribution of h_p/h_t to the total heat transfer falls rapidly with increasing U/U_{mf} in the static regime and tends to a fairly stable value in the dynamic regime (Fig. 10).

The mean h_p/h_t values in the dynamic regime vary between 0.04 and 0.17 as the particle size ration d_L/d_p increases between 8 and 30 (Fig. 11). The increase of h_p/h_t with $d_L/\bar{d}_p$ can be interpreted in terms of an increase in the available contact area [5] or an increase in the population density of the fines in the stagnant gas film.

6. CONCLUSION

Relatively small quantities of large bodies immersed in fluidized beds of fine particles exhibit two distinct hydrodynamic regimes with different heat and mass transfer characteristics.

At low gas velocities ($U_{mf} < U < U_{mc}$), the large particles remain packed in an incipient bubbling bed. As U/U_{mf} increases in this 'static regime' the total heat transfer and the gas-convective mass transfer coefficients increase whereas the contribution of the interparticle heat transfer component to the overall heat transfer, h_p/h_t, decreases.

At high gas velocities ($U > U_{mc}$), the large particles circulate freely in a well-developed bubbling bed: the 'dynamic regime'. The large and fast bubbles present at this stage play a vital role in the large particle mobility. The transfer coefficients h_t and k and the ratio h_p/h_t are nearly constant in this regime.

As the large particle size decreases the total heat and convective mass transfer rates increase. A similar variation in the fine particle size favours only the total heat transfer through its positive effect on the interparticle heat transfer component.

The interparticle heat transfer contribution to the overall heat transfer increases (4–17%) in the dynamic regime as the large-to-fine particles size ratio increases between 8 and 30.

The observed heat and mass transfer characteristics are similar to those abundantly reported for bed-to-fixed surface transfer phenomena. These similarities are expected to give valuable insight in the transfer mechanisms in the studied system, which in conjunction with the findings of the mixing and segregation studies could serve as a sound basis for the rational design of processes employing this gas–solid contacting technique.

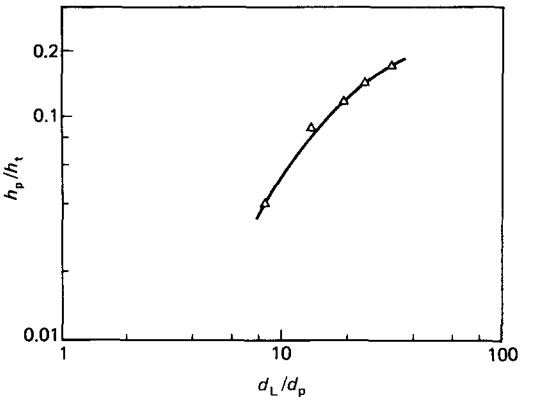

FIG. 11. Effect of the large-to-fine particle size ratio on the contribution of the interparticle heat transfer to the total heat transfer.

REFERENCES

1. J. S. M. Botterill, *Fluid-bed Heat Transfer*, pp. 145–228. Academic Press, London (1975).
2. N. I. Gelperin and V. G. Einstein, *Heat Transfer in Fluidization* (Edited by J. Davidson and D. Harrison), pp. 471–540. Academic Press, London (1971).
3. H. S. Mickley and D. F. Fairbanks, Mechanism of heat transfer to fluidized beds, *A.I.Ch.E. Jl* **1**, 374–384 (1955).
4. J. S. M. Botterill, K. A. Reddish, D. K. Ross and J. R. Williams, The mechanism of heat transfer to fluidized beds, *Proc. Symposium on Interaction Between Fluids and Particles*, London, pp. 183–189 (1962).
5. C. Y. Wen and T. M. Chang, Particle-to-particle heat transfer in air fluidized beds, *Proc. Int. Symposium on Fluidization*, Eindhoven, pp. 491–506 (1967).
6. J. Vanderschuren and C. Delvosalle, Particle-to-particle heat transfer in fluidized bed drying, *Chem. Engng Sci.* **35**, 1741–1748 (1980).
7. S. Sugiyama, M. Hasatani and M. Nakamura, Effects of surface resistances on simultaneous heat and mass transfer in porous solids with phase change, *Int. J. Heat Mass Transfer* **17**, 899–907 (1974).
8. G. M. Rios and H. Gilbert, Heat transfer between gas fluidised bed and big bodies: analysis and explanation of big body mobility effects, *4th Int. Conference on Fluidization*, Japan, Paper No. 5–7 (1983).
9. P. N. Rowe and A. W. Nienow, Particle mixing and segregation in gas fluidised beds, *Rev. Powder Technol.* **15**, 141–147 (1976).
10. E. N. Ziegler and W. I. Brazetton, Mechanism of heat transfer to a fixed surface in a fluidized bed, *I.E.C. Fund.* **3**, 94–98 (1964).
11. T. Shirai, H. Yoshitome, Y. Shoji, K. Hojo and S. Yoshida, Heat and mass transfer on the surface of solid spheres sixed within fluidised, *Kagaku Kogaku* (*Chem. Engng Japan*) **29**, 880–884 (1965).
12. E. N. Ziegler and J. T. Holmes, Mass transfer from fixed surfaces to gas fluidized beds, *Chem. Engng Sci.* **21**, 117–122 (1966).
13. D. Steinmetz, D. Barreteau and C. Laguérie, Transfert de chaleur entre une sphère fixe et un lit fluidisé entre 150 et 1000°C, *3èmes Journées Européennes sur la Fluidisation*, Compiègne, pp. 82–89 (1983).